Published in final edited form as:

Immunohorizons. 2018 December ; 2(11): 384–397. doi:10.4049/immunohorizons.1800063.

Mitochondria Released by Apoptotic Cell Death Initiate Innate Immune Responses

Minghua Zhu[*,1], **Andrew S. Barbas**[*,1], **Liwen Lin**[*,1], **Uwe Scheuermann**[*], **Muath Bishawi**[*], and **Todd V. Brennan**[†]

[*]Department of Surgery, Duke University Medical Center, Durham, NC 27710

[†]Department of Surgery, Cedars-Sinai Medical Center, Los Angeles, CA 90048

Abstract

In solid organ transplantation, cell death arising from ischemia/reperfusion leads to the release of several damage-associated molecular patterns derived from mitochondria. Mitochondrial damage-associated molecular patterns (mtDAMPs) initiate proinflammatory responses, but it remains unknown whether the mode of cell death affects the inflammatory properties of mitochondria. Murine and human cell lines induced to selectively undergo apoptosis and necroptosis were used to examine the extracellular release of mitochondria during programmed cell death. Mitochondria purified from healthy, apoptotic, and necroptotic cells were used to stimulate macrophage inflammasome responses in vitro and neutrophil chemotaxis in vivo. Inhibition of specific mtDAMPs was performed to identify those responsible for macrophage inflammasome activation. A rat liver transplant model was used to identify apoptotic and necroptotic cell death in graft tissue following ischemia/reperfusion. Both apoptotic and necroptotic cell death occur in parallel in graft tissue. Apoptotic cells released more mitochondria than necroptotic cells. Moreover, mitochondria from apoptotic cells were significantly more inflammatory in terms of macrophage inflammasome activation and neutrophil recruitment. Inhibition of cellular synthesis of cardiolipin, a mitochondria-specific lipid and mtDAMP, significantly reduced the inflammasome-activating properties of apoptosis-derived mitochondria. Mitochondria derived from apoptotic cells are potent activators of innate immune responses, whereas mitochondria derived from healthy or necroptotic cells are significantly less inflammatory. Cardiolipin appears to be a key mtDAMP-regulating inflammasome activation by mitochondria. Methods of inhibiting apoptotic cell death in transplant grafts may be beneficial for reducing graft inflammation and transplant allosensitization.

Address correspondence and reprint requests to: Dr. Andrew S. Barbas, Duke University Medical Center, Duke University Medical Center Box 3512, Durham, NC 27710. andrew.barbas@duke.edu.

[1]M.Z., A.S.B., and L.L. contributed equally.

DISCLOSURES

The authors have no financial conflicts of interest.

The online version of this article contains supplemental material.

INTRODUCTION

Cell injury and death occur during multiple phases of the transplant process as an organ moves from donor to recipient (1). The initial injury occurs in the donor, as organs are exposed to an inflammatory milieu associated with brain death pathophysiology (2–4). After organ procurement, grafts become further injured during anoxic cold storage and at the time of reperfusion because of ischemia/reperfusion pathophysiology (5). This cumulative injury leads to cell death in the transplanted graft. However, the pathways by which cell death occurs, the inflammatory nature of the cell death, and the molecules responsible for the inflammatory response remain poorly understood.

Cell death results in the release of a heterogeneous group of molecules collectively referred to as damage-associated molecular patterns (DAMPs) (6, 7). DAMPs subsequently bind to pattern recognition receptors and trigger innate immune inflammatory responses, potentially creating a feed-forward cycle that can lead to further cell injury. To date, multiple DAMPs have been identified that are derived from damaged cells and extracellular matrix (8–10). Mitochondria, evolutionarily derived from bacteria (11, 12), are known to be the source of multiple cellular DAMPs (13–16). Mitochondrial DAMPs (mtDAMPs) include ATP, mitochondrial DNA (mtDNA), reactive oxygen species (ROS), N-formylated peptides, and cardiolipin. In addition to these canonical DAMPs, there is growing evidence that intact mitochondria released from dying cells may themselves have proinflammatory properties (17).

We hypothesized that mitochondria from dying cells have distinct inflammatory properties, depending on the pathway of cell death. To test this hypothesis, we used mouse and human cell lines to examine the release of mitochondria during regulated cell death (apoptosis and necroptosis) and to investigate the inflammatory properties of these mitochondria. We demonstrate that mitochondria from apoptotic cells are potent activators of the NLRP3 inflammasome, resulting in IL-1β production and causing neutrophil recruitment. In contrast, mitochondria purified from healthy cells or necroptotic cells lacked these properties. Cardiolipin was identified as a key molecule involved in inflammasome activation by mitochondria from apoptotic cells. Using a rodent model of liver transplant, we demonstrate the occurrence of both pathways of programmed death during organ storage and reperfusion. These findings have implications for reducing innate immune activation in transplantation and in other settings of sterile inflammation.

MATERIALS AND METHODS

Rat liver transplant model

Rat livers were isolated and preserved for 4 h by either static cold storage consisting of immersion in University of Wisconsin preservation solution (Bridge of Life, Columbia, SC) at 4°C or by normothermic machine perfusion at 37°C. In the normothermic machine perfusion group, circulating perfusate consisted of an oxygenated mixture of Williams Medium E (Sigma-Aldrich, St. Louis, MO) supplemented with 5% BSA (GE Healthcare Life Sciences, South Logan, UT) and human RBCs to a hematocrit of 10–15%. Additives included 500 U of heparin (Fresenius Kabi, Lake Zurich, IL), 0.2U of regular insulin (Eli

Lilly and Company, Indianapolis, IN), and 1 mg of hydrocortisone (Pharmacia and Upjohn, Division of Pfizer, New York, NY). Following the 4 h organ storage period, simulated transplantation was performed by reperfusion of the graft at 37°C using oxygenated Krebs–Henseleit buffer (Sigma-Aldrich) for a period of 2 h, as previously described (18).

Cell lines

The L929 (mouse fibroblast) and J774A.1 (mouse monocyte) cell lines were purchased from the American Type Culture Collection (Manassas, VA). Both cell lines were maintained in a 5% CO_2 atmosphere at 37°C in DMEM supplemented with 10% heat-inactivated FBS and penicillin/streptomycin. L929 cells with DsRed fluorescently labeled mitochondria were produced by expanding a stable clone from L929 cells transduced with the mitochondrial-targeted DsRed lentiviral vector, pLV-mitoDsRed, a gift from P. Tsoulfas (19) (Addgene plasmid no. 44386). Mouse peritoneal macrophages were harvested from mouse peritoneal cavities 3 d following the i.p. administration of 1 ml of 3% (w/v) thioglycolate medium (Thermo Fisher Scientific), as previously described (20).

Jurkat cells (human T cell) and FADD-deficient ($FADD^{-/-}$) Jurkat cells were purchased from American Type Culture Collection. RIP1-deficient ($RIP1^{-/-}$) Jurkat cells were a kind gift from Dr. B. Seed (21) (Massachusetts General Hospital, Cambridge, MA). Jurkat cell lines were maintained in a 5% CO_2 atmosphere at 37°C in RPMI 1640 containing 10% heat-inactivated FBS, penicillin/streptomycin (100 U/ml each), 55 μM 2-ME, and 10 μM HEPES.

Cell death induction

L929 cells were treated with 1 μM staurosporine (STA; Abcam, Cambridge, MA) to induce apoptosis or with TZS, consisting of 12.5 ng/ml TNF-α (Enzo Life Sciences, Farmingdale, NY), 20 μM Z-VAD–fmk (Enzo Life Sciences), and 100 nM SMAC mimetic (Birinapant; Chemietek, Indianapolis, IN) to induce necroptosis. $RIP1^{-/-}$ or $FADD^{-/-}$ Jurkat cells were treated with human TNF-α (50 ng/ml; Enzo Life Sciences), for 6–20 h and then stained with annexin V and 7-aminoactinomycin D (7-AAD) using annexin V binding buffer (BD Biosciences, San Jose, CA), at 4°C for 30 min. To confirm the specificity of cell death for $RIP1^{-/-}$ or $FADD^{-/-}$ Jurkat cells, cells were treated with 20 μM Z-VAD–fmk (Enzo Life Sciences) or 50 μM necrostatic-1 (Nec-1; Cayman Chemical, Ann Arbor, MI), inhibitors of apoptosis and necroptosis, respectively.

Tissue lysates

Rat livers were flash frozen in RNAlater (Thermo Fisher Scientific, Waltham, MA) at −80°C. Protein from liver pieces were then extracted using cell disruption buffer from PARIS Kit (Thermo Fisher Scientific).

Cell lysates

Cell lines were harvested and lysed in ice-cold radioimmunoprecipitation assay lysis buffer in the presence of proteinase inhibitor mixture (Sigma-Aldrich), 1 mM PMSF (Santa Cruz Biotechnology, Dallas, TX), 10 mM sodium fluoride (Sigma-Aldrich), and 1 mM sodium orthovanadate (Sigma-Aldrich).

Western blot analysis

Total protein from each sample (10–20 μg) was separated by SDS-PAGE and transferred to nitrocellulose membranes (Bio-Rad Laboratories, Hercules, CA). Abs used for protein detection were the following: anti–poly(ADP-ribose) polymerase (PARP) (product no. 9542S; Cell Signaling Technology, Danvers, MA), anti–mixed lineage kinase domain-like pseudokinase (MLKL) phospho-S345 (product no. ab196436; Abcam), anti-GAPDH (product no. ab181602; Abcam), anti-HSP70 (product no. 610607; BD Biosciences), and anti-ATP5a (product no. ab176569; Abcam). Western blot membranes were stripped of Abs using Restore Plus Western Blot Stripping Buffer (Thermo Fisher Scientific) when additional Ab probing was required.

Cell death analysis, mitochondrial membrane potential, and ROS generation assay

Cell death was assessed by dual staining with annexin V and 7-AAD, which were performed using the PE Annexin V Apoptosis Detection Kit I (no. 559763; BD Biosciences) at 4°C for 30 min. Mitochondrial membrane potential was assessed by treating cells with 25 nM DiOC6 (Enzo Life Sciences) or 100 nM MitoTracker Green and 100 nM MitoTracker Red (Thermo Fisher Scientific) at room temperature for 30 min. Cells were incubated with 1 μM MitoSOX Red (Thermo Fisher Scientific) at room temperature for 30 min to measure ROS levels. Carbonyl cyanide *m*-chlorophenylhydrazone (CCCP; 50 μM; Sigma-Aldrich) was used as a positive control for inducing membrane depolarization.

Isolation of mitochondria and mtDNA

L929 cells (1×10^8) were harvested, and cell pellets were washed two to three times with PBS at 4°C, resuspended in 1 ml Isolation Buffer for Cells (IBC) (10 mM Tris-MOPS [pH 7.4], 1 mM EGTA/Tris [pH7.4], and 0.2 M sucrose) and passed through a 27-G needle 10–20 times. An additional 4 ml of cold Isolation Buffer for Cells (IBC) was added, and the homogenate was centrifuged at 700×*g* for 10 min at 4°C. The resulting supernatant (SN) was then centrifuged again at 700 × *g* for 10 min, and SN was collected and centrifuged once more at 12,000×*g* for 10 min at 4°C. The pellet, consisting predominantly of mitochondria, was then resuspended with PBS at 4°C. Mitochondrial protein concentration was measured by Bradford reagent (Sigma-Aldrich). mtDNA was purified from isolated mitochondria using the QIAamp DNA Blood Mini Kit (Qiagen, Germantown, MD). Oxidative damage to mtDNA was assessed by measuring 8-hydroxydeoxyguanosine (8-OHdG) levels by ELISA (StressMarq Biosciences, Victoria, BC, Canada).

Lipid extraction from purified mitochondria

Mitochondria were isolated from apoptotic L929 cells and resuspended in PBS. They were then mixed with 1 vol of chloroform and 2 vol of methanol as previously described (22). The mixture was homogenized by vortexing for 30 s and then centrifuged at 1000 × *g* for 10 min at room temperature. After centrifugation, the top aqueous layer (enriched for DNA or water-soluble components), interface (enriched for denatured proteins), and bottom chloroform layer (enriched for lipids) were collected. The lipid layer containing chloroform was dried in a sterile hood and resuspended in sterile PBS.

Cytokine production and caspase-1 activity

J774A.1 cells were primed with LPS (100 ng/ml) for 4–6 h and then stimulated with purified mitochondria(100 μg/ml) for 16 h. IL-1β, IL-6, and TNF-α production by J774A.1 cells was measured by FACS using Cytometric Bead Assays (BD Biosciences). Caspase-1 activity in SNs was measured using the Caspase-Glo 1 Inflammasome Assay (Promega, Madison, WI).

Peritoneal exudate cell assay

The peritoneal exudate cell (PEC) assay was performed as previously described (23). Briefly, C57BL/6 mice underwent i.p. injection with either 300 μg of freshly isolated mitochondria in 200 μl of sterile PBS, 100 μg zymosan (Sigma-Aldrich) in 200 μl PBS (positive control), or 200 μl PBS alone (negative control). Eighteen hours after injection, mice were euthanized by CO_2 asphyxiation, and their peritoneal cavities were washed by injecting 5 ml of sterile PBS. The peritoneal wash was collected, and PEC neutrophils were quantified as $Ly6G^+Ly6B.2^+$ cells by FACS, gating on live cells using the Fixable Blue Dead Cell Staining Kit (Thermo Fisher Scientific).

Mitochondrial release

To determine whether human Jurkat cells also release mitochondria during cell death, we collected the microparticles from SN and then stained them with MitoTracker Deep Red (DR Thermo Fisher Scientific) and with anti-translocase of outer mitochondrial membrane 22 (TOMM22) (ab210047; Abcam) prior to FACS analysis. Mitochondria release into the cell SN was also confirmed by Western blot for the mitochondrial specific protein ATP5a (ab176569; Abcam).

mtDAMP inhibition

MitoTEMPO (10 μM; Sigma-Aldrich), an ROS inhibitor, was added to L929 culture 1 d prior to induction of apoptosis of L929 cells with STA. Apyrase (100 U/ml) or DNase (200 μg/ml), both from Sigma-Aldrich, were added to the purified mitochondria at 37°C for 30 min. Palmitate or oleate (0.5 mM dissolved in 0.1 N NaOH/12% BSA at a 1:9 ratio), both from Sigma-Aldrich, were added to L929 culture in serum-free medium for 1 d prior to induction of apoptosis of L929 cells with STA.

Quantification of cardiolipin from purified mitochondria

Mitochondria were isolated from apoptotic L929 cells pretreated with 0.5 mM palmitate or oleate, as described above. A Cardiolipin Assay Kit (no. K944; BioVision, Milpitas, CA) was used to determine cardiolipin concentration in the mitochondrial preparation. Fluorescence was recorded at excitation/emission 355/460 nm for the measurement of cardiolipin.

Confocal microscopy

Images were acquired using a Leica SP5 AOBS confocal microscope (Leica Microsystems) equipped with a 40× (1.25 NA) oil immersion objective. Four hundred five–nanometer and five hundred sixty-one–nanometer lasers were used to excite DAPI and DsRed, respectively.

Sequential acquisition of the multicolor images was used to avoid cross-excitation, and images were overlaid with the Leica LAS AF 2.6 software.

Electron microscopy of mitochondria

Mitochondria were obtained either from treated cells or microparticles from SNs of cell cultures. Thin sections were obtained from purified mitochondria fixed with 3% glutaraldehyde in 0.1 M cacodylic acid buffer (pH 7.4) (Ladd Research Industries, Williston, VT). The samples were washed three times with 0.1 M cacodylic acid buffer and poststained with 1% osmium tetroxide in cacodylic buffer for 1 h. Cells were then washed and embedded in 1% agarose. The agarose containing the cell sample was then prestained with 2% uranyl acetate (Polaron Instruments, Hatfield, PA) overnight at 4°C. The samples were washed and carried through acetone dehydration steps. Infiltration was done using the Epon-Embedding Kit (Electron Microscopy Sciences, Hatfield, PA). Samples were ultrathin sectioned (60–70 nm) on a Reichert Ultracut E Ultramicrotome, and sections were stained with 2% uranyl acetate in 50% ethanol for 30 min and SATO lead stain for 1 min. Samples were imaged on a Philips CM12 electron microscope.

Statistical analysis

The p values were obtained from Mann–Whitney U test for unpaired data. For multiple comparisons, Kruskal–Wallis with Dunn multiple comparison tests were performed. Two-tailed p values <0.05 were considered significant. Analyses were performed using GraphPad Prism 7 software.

RESULTS

Cells undergoing apoptosis and necroptosis secrete intact mitochondria

L929 cells were used to study the effects of apoptosis and necroptosis on mitochondrial release. Treatment of L929 cells with STA (1 mM) specifically caused apoptosis, whereas treatment with a combination of TNF-α (12.5 ng/ml), Z-VAD (20 mM; a pan-caspase inhibitor), and a SMAC mimetic (Birinapant; 100 nM) specifically caused necroptosis. Specificity for programmed cell death pathways was demonstrated by performing Western blots of cell lysates and probing for cleaved PARP or pMLKL, specific markers for apoptosis and necroptosis, respectively. As shown in Fig. 1A, STA and TZS treatments specifically induced apoptotic and necroptotic programmed cell death, respectively. FACS analysis for annexin V binding and 7-AAD uptake of L929 cells treated for 4 h with STA or TZS was also consistent with apoptosis and necroptosis, respectively (Fig. 1B). Examination of the time course of cell death induced in L929 cells by STA and TZS, as phenotyped by FACS staining for annexin V and 7-AAD, showed that STA treatment resulted in ~75% cell death by 20 h, and TZS treatment resulted in .90% cell death by 4 h (Fig. 1C).

To test whether cells undergoing programmed cell death secrete mitochondria, we developed an L929 cell line that stably expresses mitochondrial-targeted DsRed fluorescent protein. We then induced cell death by treatment with STA (20 h) or TZS (4 h) and performed FACS analysis of the subcellular particles in the cell culture SN. The subcellular debris, or microparticles, were purified from the SN by differential centrifugation to first remove

whole cells and then to pellet the microparticles. Gating on the DsRed$^+$ microparticles in the SN demonstrated that ~75% of the microparticles from the apoptotic cell SN were DsRed$^+$ and ~40% of the microparticles purified from the necroptotic SN were DsRed$^+$ (Fig. 1D). Enumeration of the DsRed microparticles per milliliter of cell culture SN obtained from treated confluent tissue culture flasks showed that apoptosis also resulted in ~6-fold greater release of DsRed-labeled microparticles (Fig. 1E). These microparticles could represent whole mitochondria, mitochondrial fragments, or mitochondrial fragments fused to other membranous organelles. To better understand their nature, we performed scanning electron microscopy on the pelleted microparticles in the SN (Supplemental Fig. 1). We found that following apoptosis, damaged appearing (swollen, fragmented, and loss of cristae structure) extracellular mitochondria were frequently contained in membrane-bound vesicles. In contrast, following necroptosis, extracellular damaged appearing mitochondria were not within membrane structures.

Mitochondria from apoptotic and necroptotic cells are internalized by macrophages and differentially affect inflammasome activation

It has been previously demonstrated that mitochondria play a role in the activation of the NLRP3 inflammasome (24). We sought to test whether mitochondria from healthy, apoptotic, or necroptotic cells have differential effects on NLRP3 inflammasome activation. First, we isolated mitochondria from healthy, apoptotic, and necroptotic L929 cells containing DsRed-labeled mitochondria and then incubated these mitochondria with J774A.1 cells, a well-established mouse macrophage cell line used for studying inflammasome activation. FACS analysis of the macrophages showed that all three types of mitochondria associated with these cells (Fig. 2A). Internalization of the DsRed-mitochondrial by J774A.1 cells was then demonstrated by confocal microscopy (Fig. 2B).

NLRP3 activation of LPS-primed macrophages leads to the production and secretion of IL-1β. To test if the mitochondria caused inflammasome activation, LPS-primed J774A.1 or primary peritoneal macrophages were treated with mitochondria purified from healthy, apoptotic, or necroptotic L929 cells. Interestingly, only mitochondria derived from apoptotic cells resulted in IL-1β production by both J774A.1 cells and primary peritoneal macrophages (Fig. 2C, 2D). ATP (5 mM) was used as a positive control for inflammasome activation.

Caspase-1 is a proteolytic subunit of the active NLRP3 inflammasome that cleaves the IL-1β precursor to produce secreted IL-1β. To provide further evidence that apoptotic mitochondria caused NLRP3 inflammasome activation, we analyzed caspase-1 activation by purified mitochondria in LPS-primed J744A.1 macrophages (Fig. 2E). We found that only mitochondria from apoptotic cells, but not from healthy or necroptotic cells, caused caspase-1 activation. ATP was used as a positive control for inflammasome activation.

Using unprimed J774A.1 cells, we then examined the production of IL-6 and TNF-α caused by treatment with purified mitochondria. Only apoptotic mitochondria caused IL-6 production (Fig. 2F). None of the mitochondria lead to TNF-α production (Fig. 2G). Treatment with LPS (100 ng/ml) was used as a positive control for IL-6 and TNF-α production.

Mitochondria from apoptotic cells recruit neutrophils in vivo

Inflammasome activation leads to the production of proinflammatory cytokines and the recruitment of immune cells, such as neutrophils. To assess whether mitochondria from healthy, apoptotic, and necroptotic cells induce differential acute inflammatory responses in vivo, mitochondria from L929 cells were injected into the peritoneal cavity in C57BL/6 mice. Neutrophil recruitment into the peritoneal cavity was assessed 18 h after injection by FACS analysis of the PECs. Neutrophils were identified as $Ly6G^{+}Ly6B.2^{+}$ cells as previously described (23). Representative FACS plots of PECs obtained after i.p. injection of PBS (vehicle control), zymosan (positive control), and mitochondria purified from healthy, apoptotic, and necroptotic cells are shown in Fig. 3A. The summary for six mice per group is shown in Fig. 3B. Whereas all three types of mitochondria led to significant increases in neutrophil influx, apoptotic mitochondria induced the greatest PEC neutrophil recruitment.

Apoptosis and necroptosis produce dysfunctional mitochondria

To investigate the functional state of mitochondria released by apoptotic and necroptotic cells, we measured mitochondrial membrane potential, ROS production, and mtDNA oxidative damage in healthy, apoptotic, and necroptotic L929 cells. L929 cells were treated with STA for 20 h or TZS for 6 h to induce apoptosis and necroptosis, respectively. The mitochondrial membrane potential was then measured by costaining with MitoTracker Green and MitoTracker Red. MitoTracker Green localizes to mitochondria independent of the mitochondrial membrane potential, whereas MitoTracker Red accumulation within mitochondria is dependent on the membrane potential. CCCP, an uncoupler of mitochondrial oxidative phosphorylation, abolishes the mitochondrial membrane potential and was used as a control. We found that both apoptosis and necroptosis lead to significant loss of mitochondrial membrane potential (Fig. 4A). This finding was confirmed using DiOC6, a green fluorescent dye that is also dependent on mitochondrial membrane for uptake and accumulation within mitochondria (Fig. 4B).

To assess mitochondrial ROS production, we stained healthy, apoptotic, and necroptotic L929 cells with MitoSOX Red, an indicator of mitochondrial superoxide production. We found that superoxide production was enhanced in both apoptotic and necroptotic mitochondria relative to healthy mitochondria (Fig. 4C).

We next examined oxidative damage to mtDNA by measuring the accumulation of 8-OHdG levels in purified mtDNA. As shown in Fig. 4D, 8-OHdG levels were significantly increased in mitochondria from apoptotic L929 cells compared with mitochondria from either healthy or necroptotic cells. This result indicates that whereas both apoptotic and necroptotic mitochondria are dysfunctional, apoptotic mitochondria accumulate greater DNA damage.

Mitochondrial cardiolipin plays a critical role in inflammasome activation

To ascertain which components of apoptotic mitochondria are responsible for the observed inflammasome activation, we began by exposing mitochondria to extremes of temperature to denature proteins and DNA. This was accomplished by heating purified mitochondria from healthy, apoptotic, or necroptotic L929 cells at 100°C for 5 min or by freezing them at −80°C for 2 h (Fig. 5A). We found that the ability of apoptotic mitochondria to stimulate

IL-1β production in LPS-primed J744A.1 cells remained intact after exposure to both temperature extremes, indicating temperature stability of the inflammasome-activating component (Fig. 5A).

Next, we performed a transwell assay to physically separate the apoptotic mitochondria from the J744A.1 cells using a 0.4-μM transwell filter. This filter size should physically segregate intact mitochondria, which generally vary in size from between 0.5 and 2 μm. We found that the transwell barrier significantly reduced IL-1β production by LPS-primed J744A.1 cells treated with apoptotic mitochondria, suggesting that intact mitochondria or large mitochondrial fragments contributed to the inflammasome response (Fig. 5B).

ROS (25), ATP (26), and oxidized mtDNA (27) are mtDAMPs that have been shown to cause NLRP3 inflammasome activation. We thus examined whether inhibiting these molecules would prevent inflammasome activation by apoptotic mitochondria. To inhibit ROS, we incubated L929 cells with MitoTEMPO during the induction of apoptosis with STA. To inhibit ATP and mtDNA, we treated purified apoptotic mitochondria with apyrase (an ATPase) and DNAse, respectively. Interestingly, none of these treatments affected the ability of apoptotic mitochondria to activate the inflammasome, suggesting that neither ROS, ATP, nor mtDNA were critical to this mechanism (Fig. 5C).

Cardiolipin is a lipid mtDAMP that has recently been shown to also activate the NLRP3 inflammasome (24). Cardiolipin is a phospholipid normally located in the inner mitochondrial membrane that becomes externalized to the outer mitochondrial membrane surface following mitochondrial damage, where it serves as a signal for mitophagy (28). To examine the role that lipid mtDAMPs play in inflammasome activation by mitochondria, we performed a chloroform lipid extraction of mitochondria purified from apoptotic cells. The chloroform-soluble fraction enriched in lipids, and the aqueous fraction enriched in proteins and DNA, were tested against LPS-primed J744A.1 cells. Interestingly, the chloroform fraction retained the majority of the IL-1β stimulating activity, suggesting that the inflammasome-activating component in these mitochondria was a lipid (Fig. 5D).

Cellular cardiolipin synthesis is inhibited by treatment with the saturated long chain fatty acid palmitate (C16:0), but not by the monounsaturated fatty acid oleate (C18:1) (24, 29). To ascertain whether cardiolipin from apoptotic mitochondria was involved in inflammasome activation, we treated L929 cells with palmitate or oleate (negative control) prior to the induction of apoptosis. We then induced apoptosis and measured the concentration of cardiolipin in the mitochondrial preparation of these apoptotic cells. The cardiolipin concentration was significantly lower in the mitochondrial preparation from palmitate-treated cells in comparison with oleate-treated cells (Fig. 5E). Mitochondria purified from these cells were then used to treat LPS-primed J774A.1 macrophages and IL-1β production was measured. As shown in Fig. 5F, apoptotic mitochondria derived from cells that were pretreated with palmitate were significantly less inflammatory. Decreased IL-1β production by J774A.1 macrophages correlated directly with decreased levels of cardiolipin in the mitochondrial preparation.

Human T cells also release mitochondria during apoptosis and necroptosis, and apoptotic mitochondria recruit neutrophils in vivo

We next tested whether our finding with mouse cells would be recapitulated in human cells. For this purpose, we used RIP1$^{-/-}$ and FADD$^{-/-}$ Jurkat cell lines (human T cells). Both cell lines are stimulated to undergo cell death by the same molecule, TNF-α. However, the RIP1$^{-/-}$ Jurkat cells only undergo apoptosis, and the FADD$^{-/-}$ Jurkat cells only undergo necroptosis. This is demonstrated in Fig. 6A, in which the necroptosis inhibitor, Nec-1, selectively inhibits TNF-α–induced cell death in RIP1$^{-/-}$ Jurkat cells, and in Fig. 6B, in which the apoptosis inhibitor, zVAD, selectively inhibits TNF-α–induced cell death in FADD$^{-/-}$Jurkat cells.

To determine whether Jurkat cells also release mitochondria during cell death, microparticles from cell culture SN were collected by centrifugation following TNF-α treatment. Western blot analysis was performed on the microparticle lysate for ATP5a. We found that ATP synthase subunit α (ATP5a), a mitochondria-specific protein, was present in the microparticles from both apoptotic and necroptotic Jurkat cells after 12 h of TNF-α treatment (Fig. 6B). The purified microparticles were then FACS analyzed for uptake of a mitochondria-specific dye, MitoTracker DR, and for an Ab against TOMM22, a mitochondrial outer membrane protein. As shown in Fig. 6C, the majority of the microparticles stained positive for MitoTracker DR and TOMM22. Taken together, these data indicate that mitochondria are released by human T cells during apoptotic and necroptotic cell death. Enumeration of the MitoTracker^{+}TOMM22^{+} microparticles released following TNF-α–induced cell death demonstrated that apoptotic death resulted in the release of more than twice the amount of mitochondrial than necroptotic death (Fig. 6D).

We next tested whether mitochondria from apoptotic and necroptotic Jurkat cells could stimulate neutrophil recruitment in vivo. C57BL/6 mice were injected i.p. with mitochondria (300 μg) purified from RIP1$^{-/-}$ or FADD$^{-/-}$ Jurkat cells that were either untreated or treated with TNF-α. An equal volume of PBS (vehicle) was injected as a negative control. Eighteen hours after injection, PECs were harvested and analyzed by FACS for Ly6G^{+}Ly6B.2^{+} neutrophils. As shown in Fig. 6E, only apoptotic mitochondria (from TNF-α–treated RIP1$^{-/-}$ Jurkat cells) resulted in significant neutrophil recruitment. These results were consistent with those found in studies of mouse cells and suggest a similar mechanism of mitochondrial damage occurs in mouse and human cells undergoing apoptosis that renders them more inflammatory.

Apoptotic and necroptotic cell death occurs during the transplant process

We next sought to determine the clinical relevance of programmed cell death occurring in the setting of organ transplantation. The transplant process consists of three phases that cause cellular injury that could result in programmed cell death within the transplant organ: 1) organ procurement from the donor, 2) organ storage outside the body, and 3) oxidative injury caused by reperfusion of the organ. The specific types of programmed cell death occurring during the transplant process are unknown. We thus sought to ascertain whether apoptosis and/or necroptosis occur in rat livers undergoing the transplant process.

To simulate clinical organ storage, we harvested rat livers from heart-beating donors and then stored the livers either using cold static storage in ice-cold preservation fluid or using normothermic (37°C) machine perfusion conditions by perfusing the livers with a mixture of RBCs and hepatocyte cell culture medium, as previously described (30). We then simulated graft reperfusion by perfusing the rat livers with oxygenated Krebs–Henseleit buffer at 37°C for a period of 2 h, as previously described (18). Protein lysates of the reperfused livers were prepared and tested by Western blot analysis for the presence of cleaved PARP or pMLKL, specific markers for apoptosis and necroptosis, respectively. Lysates of L929 cells specifically induced to undergo apoptosis with STA or necroptosis with TZS served as positive controls. As shown in Fig. 7, liver grafts preserved by either static cold storage or normothermic machine perfusion, followed by reperfusion at 37°C, demonstrated significantly higher levels of cleaved PARP and pMLKL than fresh liver tissue. These results indicates that both apoptotic and necroptotic cell death occur in parallel in graft tissue during the transplant process.

DISCUSSION

In this review, we report the novel finding that mitochondria released by dying cells have distinct effects on inflammasome activation and neutrophil recruitment in vivo, depending on the mode of regulated cell death. Specifically, mitochondria from apoptotic cells are potent activators of the NLRP3 inflammasome and neutrophil recruitment, whereas mitochondria from healthy and necroptotic cells are much less stimulatory. These findings may help explain recent observations that apoptotic cell death can be proinflammatory, contrary to previous paradigms of apoptosis as a noninflammatory process (31–34).

Under physiologic conditions, apoptotic cells and their membrane-bound cellular debris are rapidly cleared by phagocytes, thereby limiting the release of intracellular DAMPs into the extracellular milieu. However, in conditions in which apoptotic cells are not adequately cleared by phagocytes, they undergo secondary necrosis, defined by the loss of membrane integrity and the release of intracellular contents. This process is highly inflammatory, as the cellular disintegration releases DAMPs that subsequently incite proinflammatory cascades (35–37). This is relevant to the findings in our study, as apoptosis was induced in the absence of phagocytic cells and thus progressed to secondary necrosis. The mechanisms by which apoptotic mitochondria gain proinflammatory qualities during this process remains to be elucidated, but there are clinical correlates supporting this notion. Impaired clearance of apoptotic debris is a common feature of patients suffering from chronic inflammatory diseases, such as systemic lupus erythematosus (38), chronic granulomatous disease (39), and Sjogren syndrome (40).

The inflammatory properties of pathologic apoptosis have also been demonstrated in the setting of transplantation. Islets engineered to express Fas ligand to cause apoptosis of anti-islet, allospecific T cells produced a robust innate immune response leading to neutrophil infiltration and graft loss (31, 34). This finding is similar to the peritoneal neutrophil exudate that we demonstrated in response to injections of mitochondria purified from apoptotic cells. These data suggest that apoptotic death within allografts caused by graft injury during the transplant process can elicit innate immune inflammation following reperfusion.

Recent studies have demonstrated that cells undergoing necroptosis secrete intact mitochondria (17, 41, 42). Our findings represent an extension of work by Maeda and colleagues (17), who first demonstrated that cells undergoing necroptosis release mitochondria that have inflammatory properties. More recently, Spencer and colleagues (41) also demonstrated the release of intact mitochondria from cells undergoing necroptosis. In our study, we identify that apoptotic cells also release intact mitochondria and that the inflammatory properties of secreted mitochondria differ for necroptosis and apoptosis.

Our study provides supporting evidence that cardiolipin is a mediator of the inflammasome-activating properties of apoptotic mitochondria. This is consistent with findings of Iyer and colleagues (24), who demonstrated that mitochondrial cardiolipin binds to NLRP3 and acts as a potent activator of the NLRP3 inflammasome. Chu and colleagues (28) provide a possible mechanistic explanation by demonstrating that cardiolipin is externalized from the inner mitochondrial membrane to the outer mitochondrial membrane in damaged mitochondria. An outstanding question requiring further investigation is how the presentation and/or release of cardiolipin differs between necroptotic and apoptotic mitochondria.

From a translational perspective, the mechanisms of cell death occurring in the setting solid organ transplantation have not been characterized. In this study, we confirm that apoptosis and necroptosis occur simultaneously in liver grafts during the transplant process. This regulated cell death arises from cumulative injury sustained by the graft during the transplant continuum, particularly during organ storage and from ischemia/reperfusion injury following implantation in the recipient. An established body of literature indicates that the magnitude of this initial injury and the concomitant innate immune response appear to have long-term sequelae for the graft (43, 44). Grafts that sustain greater degrees of initial ischemic injury experience increased rates of immune-mediated rejection and impaired long-term graft function, highlighting the link between innate and adaptive immunity.

These observations suggest that interventions to limit or control mechanisms of cell death, or specific DAMPs released by cell death, may have therapeutic value in transplantation. A growing body of literature highlights the potential benefits of this strategy. In a mouse kidney transplant model, Lau and colleagues (45) demonstrated that donor kidneys from mice genetically deficient in receptor-interacting serine/threonine-protein kinase 3 ($RIPK3^{-/-}$), which cannot undergo necroptosis, experienced superior graft function and survival after transplant. More recently, in a rat lung transplant model, Kanou and colleagues (46) treated donors and recipients with necrostatin-1, an inhibitor of RIPK1, and demonstrated improvements in early graft function posttransplant. Based on our data, strategies aimed at reducing cellular apoptosis may have superior efficacy in improving graft outcome.

There are limitations of our study related to its design. For the mouse cell line experiments, we induced apoptosis with STA. Although this is a well-accepted and specific method of inducing apoptosis, prolonged exposure to STA can also induce other forms of programmed cell death, particularly necroptosis. We demonstrate that at 20 h, the dominant form of cell death is apoptosis, but there is also a small amount of necroptosis present. Thus,

mitochondrial preparations consisted predominantly of apoptotic mitochondria, but likely also included a small amount of necroptotic mitochondria. Second, we used L929 (mouse fibroblast) and Jurkat (human T cell) cell lines in this study, which may be less relevant to solid organ transplantation. The reason for this selection is that these are the best-described cell lines for studying pathways of cell death, and our experiments required systems of pure apoptosis and pure necroptosis provided by these cell lines. Future studies will be conducted using hepatocyte cell lines to determine if similar findings are relevant in the context of liver transplantation. Finally, our transplant model is simulated using ex vivo reperfusion techniques. It remains unknown how the processes we identified in this study may differ in vivo.

In conclusion, this study has identified that mitochondria secreted by apoptotic cells have potent proinflammatory properties, which appear to be mediated by activation of the NLRP3 inflammasome. In contrast, mitochondria secreted by necroptotic cells do not demonstrate this property. It appears that mitochondrial cardiolipin plays a significant role in producing this inflammatory response, but the differences between cardiolipin presentation and release between apoptotic and necroptotic mitochondria remain unknown. An improved understanding of how cell death occurs in the setting of transplantation may inform directed therapies that can reduce the inflammatory response against transplant grafts and ultimately improve graft survival.

Supplementary Material

Refer to Web version on PubMed Central for supplementary material.

ACKNOWLEDGMENTS

We thank Drs. Sara Miller and Ricardo Vancini for expertise in electron microscopy. We thank Dr. Ming Song for technical assistance.

This work was supported by National Institutes of Health Grant AI101263 (to T.V.B.) and the American Society of Transplant Surgeons Faculty Development Award (to A.S.B.).

Abbreviations used in this article:

7-AAD	7-aminoactinomycin D
DAMP	damage-associated molecular pattern
DR	Deep Red
MLKL	mixed lineage kinase domain-like pseudokinase
mtDAMP	mitochondrial DAMP
mtDNA	mitochondrial DNA
8-OHdG	8-hydroxydeoxyguanosine
PARP	poly(ADP-ribose) polymerase

PEC	peritoneal exudate cell
ROS	reactive oxygen species
SN	supernatant
STA	staurosporine
TOMM22	translocase of outer mitochondrial membrane 22

REFERENCES

1. Brennan TV, Lunsford KE, and Kuo PC 2010 Innate pathways of immune activation in transplantation. J. Transplant 2010: 1–8.
2. Stangl M, Zerkaulen T, Theodorakis J, Illner W, Schneeberger H, Land W, and Faist E 2001 Influence of brain death on cytokine release in organ donors and renal transplants. Transplant. Proc 33: 1284–1285. [PubMed: 11267293]
3. Murugan R, Venkataraman R, Wahed AS, Elder M, Hergenroeder G, Carter M, Madden NJ, Powner D, and Kellum JA, HIDonOR Study Investigators. 2008 Increased plasma interleukin-6 in donors is associated with lower recipient hospital-free survival after cadaveric organ transplantation. Crit. Care Med 36: 1810–1816. [PubMed: 18496370]
4. Barklin A 2009 Systemic inflammation in the brain-dead organ donor. Acta Anaesthesiol. Scand 53: 425–435. [PubMed: 19226294]
5. Ioannou A, Dalle Lucca J, and Tsokos GC 2011 Immunopathogenesis of ischemia/reperfusion-associated tissue damage. Clin. Immunol 141: 3–14. [PubMed: 21839685]
6. Kono H, and Rock KL 2008 How dying cells alert the immune system to danger. Nat. Rev. Immunol 8: 279–289. [PubMed: 18340345]
7. Rock KL, Latz E, Ontiveros F, and Kono H 2010 The sterile inflammatory response. Annu. Rev. Immunol 28: 321–342. [PubMed: 20307211]
8. Beg AA 2002 Endogenous ligands of Toll-like receptors: implications for regulating inflammatory and immune responses. Trends Immunol. 23: 509–512. [PubMed: 12401394]
9. Johnson GB, Brunn GJ, and Platt JL 2003 Activation of mammalian Toll-like receptors by endogenous agonists. Crit. Rev. Immunol 23: 15–44. [PubMed: 12906258]
10. Brennan TV, Rendell VR, and Yang Y 2015 Innate immune activation by tissue injury and cell death in the setting of hematopoietic stem cell transplantation. Front. Immunol 6: 101. [PubMed: 25852683]
11. Emelyanov VV 2003 Mitochondrial connection to the origin of the eukaryotic cell. Eur. J. Biochem 270: 1599–1618. [PubMed: 12694174]
12. Gray MW, Burger G, and Lang BF 1999 Mitochondrial evolution. Science 283: 1476–1481. [PubMed: 10066161]
13. West AP, Shadel GS, and Ghosh S 2011 Mitochondria in innate immune responses. Nat. Rev. Immunol 11: 389–402. [PubMed: 21597473]
14. Bird L 2012 Innate immunity: linking mitochondria and microbes to inflammasomes. Nat. Rev. Immunol 12: 229. [PubMed: 22402669]
15. Cloonan SM, and Choi AM 2012 Mitochondria: commanders of innate immunity and disease? Curr. Opin. Immunol 24: 32–40. [PubMed: 22138315]
16. Krysko DV, Agostinis P, Krysko O, Garg AD, Bachert C, Lambrecht BN, and Vandenabeele P 2011 Emerging role of damage-associated molecular patterns derived from mitochondria in inflammation. Trends Immunol 32: 157–164. [PubMed: 21334975]
17. Maeda A, and Fadeel B 2014 Mitochondria released by cells undergoing TNF-α-induced necroptosis act as danger signals. Cell Death Dis. 5: e1312. [PubMed: 24991764]
18. Bessems M, Doorschodt BM, Kolkert JL, Vetelainen RL,van Vliet AK, Vreeling H, van Marle J, and van Gulik TM 2007 Preservation of steatotic livers: a comparison between cold storage and machine perfusion preservation. Liver Transpl. 13: 497–504. [PubMed: 17394146]

19. Kitay BM, McCormack R, Wang Y, Tsoulfas P, and Zhai RG2013 Mislocalization of neuronal mitochondria reveals regulation of Wallerian degeneration and NMNAT/WLD(S)-mediated axon protection independent of axonal mitochondria. Hum. Mol. Genet 22: 1601–1614. [PubMed: 23314018]
20. Ray A and Dittel BN 2010 Isolation of mouse peritoneal cavity cells. J. Vis. Exp 35: e1488.
21. Ting AT, Pimentel-Muiños FX, and Seed B 1996 RIP mediates tumor necrosis factor receptor 1 activation of NF-kappaB but not Fas/APO-1-initiated apoptosis. EMBO J. 15: 6189–6196. [PubMed: 8947041]
22. Smaal EB, Romijn D, Geurts van Kessel WS, de Kruijff B, and de Gier J 1985 Isolation and purification of cardiolipin from beef heart. J. Lipid Res 26: 634–637. [PubMed: 4020303]
23. Chen CJ, Kono H, Golenbock D, Reed G, Akira S, and Rock KL2007 Identification of a key pathway required for the sterile inflammatory response triggered by dying cells. Nat. Med 13: 851–856. [PubMed: 17572686]
24. Iyer SS, He Q, Janczy JR, Elliott EI, Zhong Z, Olivier AK, Sadler JJ, Knepper-Adrian V, Han R, Qiao L, et al. 2013 Mitochondrial cardiolipin is required for Nlrp3 inflammasome activation. Immunity 39: 311–323. [PubMed: 23954133]
25. Heid ME, Keyel PA, Kamga C, Shiva S, Watkins SC, and Salter RD 2013 Mitochondrial reactive oxygen species induces NLRP3-dependent lysosomal damage and inflammasome activation. J. Immunol 191: 5230–5238. [PubMed: 24089192]
26. Amores-Iniesta J, Barberà-Cremades M, Martínez CM, Pons JA, Revilla-Nuin B, Martínez-Alarcón L, Di Virgilio F, Parrilla P, Baroja-Mazo A, and Pelegrín P 2017 Extracellular ATP activates the NLRP3 inflammasome and is an early danger signal of skin allograft rejection. Cell Rep. 21: 3414–3426. [PubMed: 29262323]
27. Shimada K, Crother TR, Karlin J, Dagvadorj J, Chiba N, Chen S, Ramanujan VK, Wolf AJ, Vergnes L, Ojcius DM, et al. 2012 Oxidized mitochondrial DNA activates the NLRP3 inflammasome during apoptosis. Immunity 36: 401–414. [PubMed: 22342844]
28. Chu CT, Ji J, Dagda RK, Jiang JF, Tyurina YY, Kapralov AA, Tyurin VA, Yanamala N, Shrivastava IH, Mohammadyani D, et al. 2013 Cardiolipin externalization to the outer mitochondrial membrane acts as an elimination signal for mitophagy in neuronal cells. Nat. Cell Biol 15: 1197–1205. [PubMed: 24036476]
29. Ostrander DB, Sparagna GC, Amoscato AA, McMillin JB, and Dowhan W 2001 Decreased cardiolipin synthesis corresponds with cytochrome c release in palmitate-induced cardiomyocyte apoptosis. J. Biol. Chem 276: 38061–38067. [PubMed: 11500520]
30. Op den Dries S, Karimian N, Westerkamp AC, Sutton ME, Kuipers J. Wiersema-Buist, Ottens PJ, Kuipers J, Giepmans BN, Leuvenink HG, et al. 2016 Normothermic machine perfusion reduces bile duct injury and improves biliary epithelial function in rat donor livers. Liver Transpl. 22: 994–1005. [PubMed: 26946466]
31. Allison J, Georgiou HM, Strasser A, and Vaux DL 1997 Transgenic expression of CD95 ligand on islet beta cells induces a granulocytic infiltration but does not confer immune privilege upon islet allografts. Proc. Natl. Acad. Sci. USA 94: 3943–3947. [PubMed: 9108084]
32. Faouzi S, Burckhardt BE, Hanson JC, Campe CB, Schrum LW, Rippe RA, and Maher JJ 2001 Anti-Fas induces hepatic chemokines and promotes inflammation by an NF-kappa B-independent, caspase-3-dependent pathway. J. Biol. Chem 276: 49077–49082. [PubMed: 11602613]
33. Nagata S 1997 Apoptosis by death factor. Cell 88: 355–365. [PubMed: 9039262]
34. Kang SM, Schneider DB, Lin Z, Hanahan D, Dichek DA, Stock PG, and Baekkeskov S 1997 Fas ligand expression in islets of Langerhans does not confer immune privilege and instead targets them for rapid destruction. Nat. Med 3: 738–743. [PubMed: 9212099]
35. Silva MT 2010 Secondary necrosis: the natural outcome of the complete apoptotic program. FEBS Lett. 584: 4491–4499. [PubMed: 20974143]
36. Vanden Berghe T, Vanlangenakker N, Parthoens E, Deckers W, Devos M, Festjens N, Guerin CJ, Brunk UT, Declercq W, and Vandenabeele P 2010 Necroptosis, necrosis and secondary necrosis converge on similar cellular disintegration features. Cell Death Differ. 17: 922–930. [PubMed: 20010783]

37. Crawford ED, and Wells JA 2011 Caspase substrates and cellular remodeling. Annu. Rev. Biochem 80: 1055–1087. [PubMed: 21456965]

38. Mahajan A, Herrmann M, and Muñoz LE 2016 Clearance deficiency and cell death pathways: a model for the pathogenesis of SLE. Front. Immunol 7: 35. [PubMed: 26904025]

39. Fernandez-Boyanapalli RF, Falcone EL, Zerbe CS, Marciano BE, Frasch SC, Henson PM, Holland SM, and Bratton DL 2015 Impaired efferocytosis in human chronic granulomatous disease is reversed by pioglitazone treatment. J. Allergy Clin. Immunol 136: 1399–1401.e3. [PubMed: 26386811]

40. Manoussakis MN, Fragoulis GE, Vakrakou AG, and Moutsopoulos HM 2014 Impaired clearance of early apoptotic cells mediated by inhibitory IgG antibodies in patients with primary Sjögren's syndrome. PLoS One 9: e112100. [PubMed: 25396412]

41. Spencer DM, Dye JR, Piantadosi CA, and Pisetsky DS 2018 The release of microparticles and mitochondria from RAW 264.7 murine macrophage cells undergoing necroptotic cell death in vitro. Exp. Cell Res 363: 151–159. [PubMed: 29291399]

42. Singh A, Periasamy S, Malik M, Bakshi CS, Stephen L, Ault JG, Mannella CA, and Sellati TJ 2017 Necroptotic debris including damaged mitochondria elicits sepsis-like syndrome during late-phase tularemia. Cell Death Discov. 3: 17056. [PubMed: 28955505]

43. Amico P 2010 Evolution of graft survival in kidney transplantation: an analysis of the OPTN/UNOS renal transplant registry. Clin. Transpl 1–15. [PubMed: 21698830]

44. Pratschke J, Wilhelm MJ, Kusaka M, Beato F, Milford EL,Hancock WW, and Tilney NL 2000 Accelerated rejection of renal allografts from brain-dead donors. Ann. Surg 232: 263–271. [PubMed: 10903606]

45. Lau A, Wang S, Jiang J, Haig A, Pavlosky A, Linkermann A, Zhang ZX, and Jevnikar AM 2013 RIPK3-mediated necroptosis promotes donor kidney inflammatory injury and reduces allograft survival. Am. J. Transplant 13: 2805–2818. [PubMed: 24103001]

46. Kanou T, Ohsumi A, Kim H, Chen M, Bai X, Guan Z, Hwang D, Cypel M, Keshavjee S, and Liu M 2018 Inhibition of regulated necrosis attenuates receptor-interacting protein kinase 1-mediated ischemia-reperfusion injury after lung transplantation. J. Heart Lung Transplant 37: 1261–1270. [PubMed: 29907500]

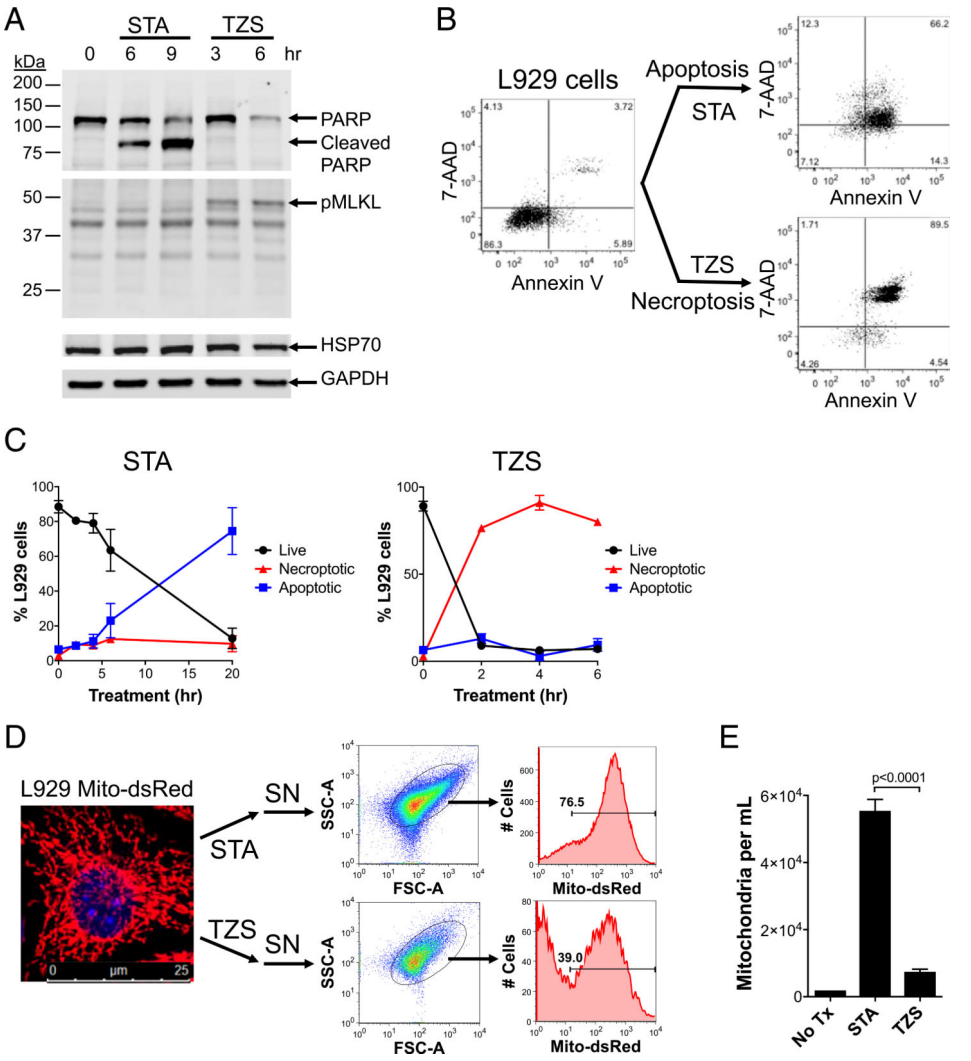

FIGURE 1. Apoptosis and necroptosis of L929 cells results in the release of mitochondria.

(**A**) Western blot analysis of L929 lysates probed with anti-PARP or anti-pMLKL Abs show a time-dependent increase in cleaved PARP following STA treatment and pMLKL following TZS treatment. Blots were reprobed with anti-HSP70 and anti-GAPDH Abs for protein loading controls. (**B**) Annexin V and 7-AAD FACS analysis of L929 cells undergoing apoptosis induced by STA treatment or necroptosis induced by TNF-α/zVAD/SMACi (TZS) treatment. L929 cells were treated with STA for 20 h or with TZS for 6 h and stained with annexin V/PE and 7-AAD. (**C**) Time course of L929 cell death following STA or TZS treatment. Live cells are annexin V^{neg}/7-AAD^{neg}, apoptotic cells are annexin V^{+}/7-AAD^{neg}, and necroptotic cells are annexin V^{+}/7-AAD^{+}. (**D**) L929 cells stably expressing mitochondrial-targeted DsRed fluorescent protein were treated with STA (20 h) or TZS (4 h). Cell culture SN was collected, and microparticles were purified by differential centrifugation and analyzed by FACS. (**E**) Quantification of extracellular DsRed-labeled mitochondria. Red staining: mitochondria stained with DsRed; blue staining: nuclei stained with DAPI. Flow cytometry image: red shading indicates mitochondria stained with DsRed. Horizontal bars indicate the percentage of microparticles containing dsRed-stained

mitochondria. Comparisons were performed using a Mann–Whitney *U* test. A *p* value <0.05 was considered significant.

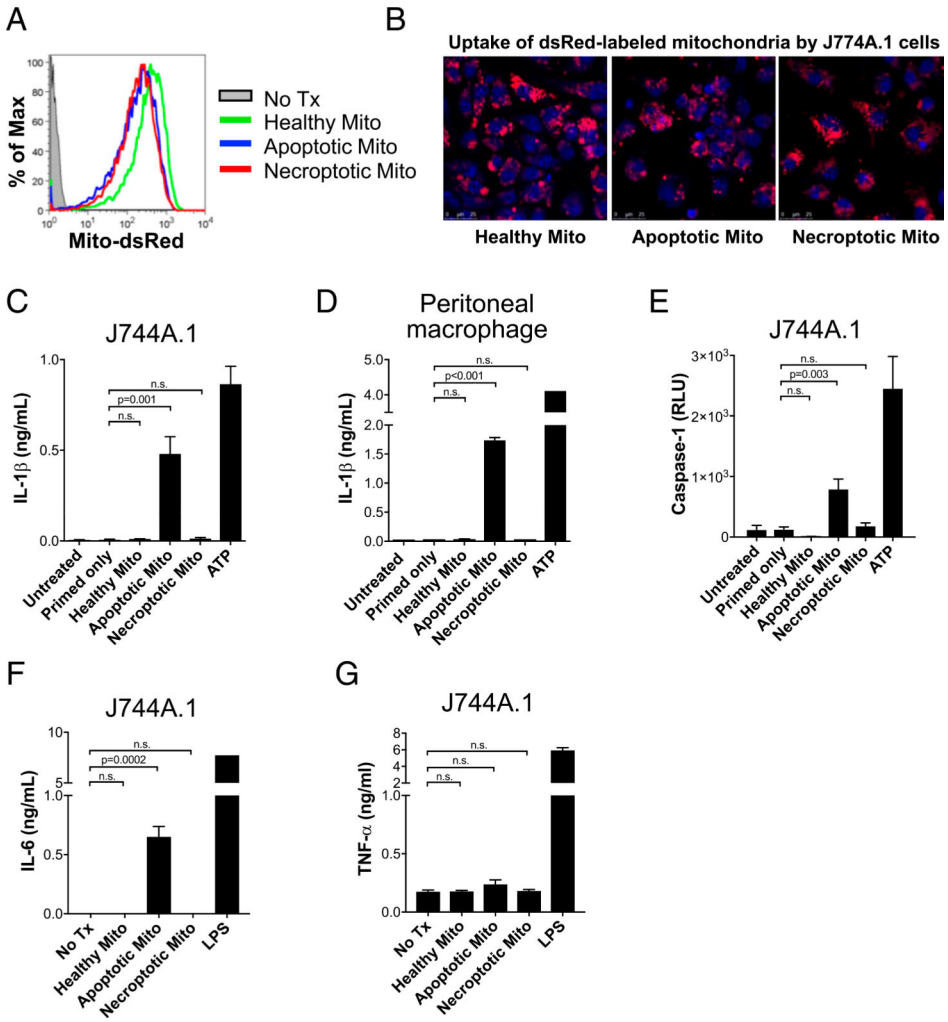

FIGURE 2. Macrophages uptake extracellular mitochondria from apoptotic cells, inducing caspase-1 activation and IL-1β production.

(**A**) J774A.1 cells were incubated with mitochondria purified from healthy, apoptotic, and necroptotic L929 cells containing DsRed-labeled mitochondria and analyzed by FACS and (**B**) imaged by confocal microscopy to confirm intracellular localization of the mitochondria. Red staining: mitochondria stained with DsRed; blue staining: nuclei stained with DAPI. Original magnification ×400. (**C**) LPS-primed J774A.1 cells were stimulated for 16 h with mitochondria (100 mg/ml) purified from healthy, apoptotic, and necroptotic L929 cells, the SN was assayed for IL-1β production, (**D**) LPS-primed primary murine (C57BL/6) peritoneal macrophages were similarly treated with mitochondria, and the SN was assayed for IL-1β. (**E**) Caspase-1 activity was measured in LPS-primed J744A.1 macrophages following treatment with purified mitochondria from healthy, apoptotic, or necroptotic cells. ATP (5 mM) served as a positive control. (**F** and **G**) Unprimed J774A.1 cells were treated with mitochondria (100 mg/ml) for 16 h, and the SN was assayed for IL-6 and TNF-α. LPS (100 ng/ml) served as a positive control. Comparisons were performed using a Kruskal–Wallis with Dunn multiple comparison test. A p value <0.05 was considered significant.

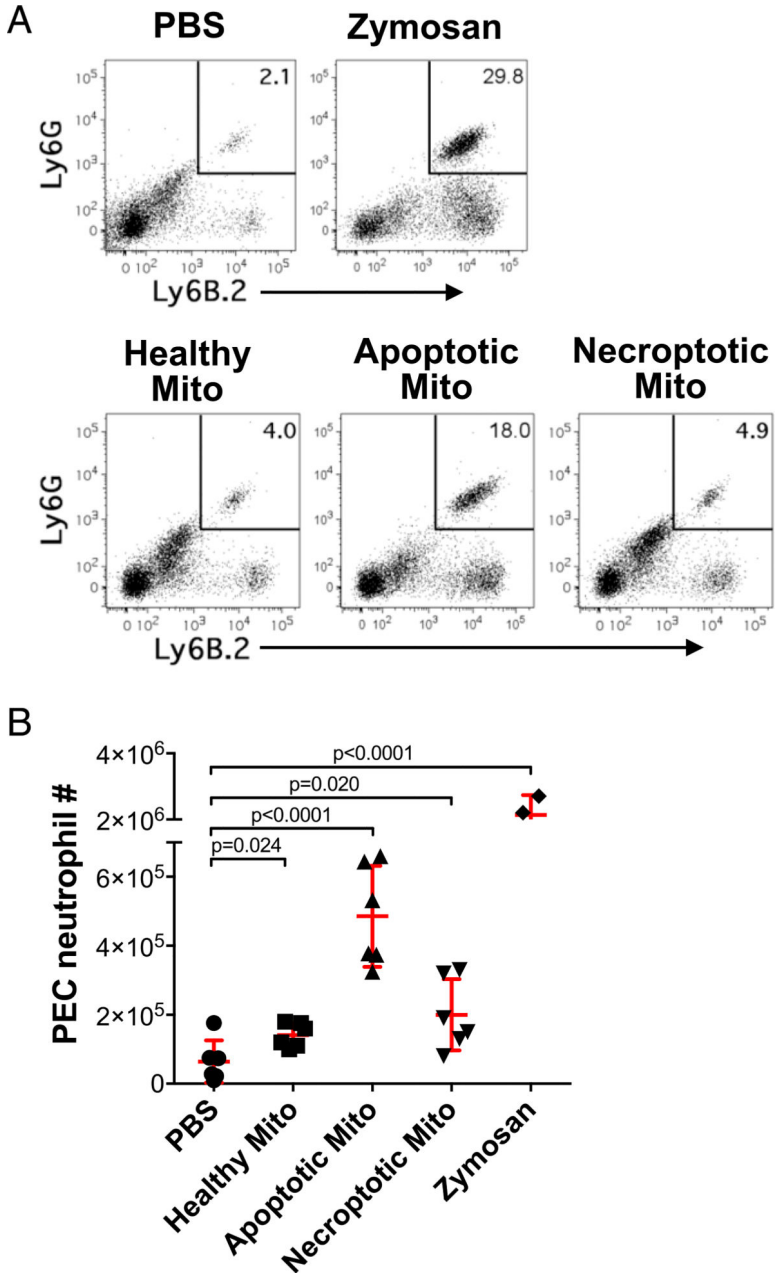

FIGURE 3. Extracellular mitochondria cause neutrophil recruitment.

(**A**) C57BL/6 mice received i.p. injections of mitochondria (300 mg) isolated from healthy, apoptotic, or necroptotic L929 cells ($n = 6$ per group), or with an equal volume of PBS (vehicle control; $n = 6$), or with zymosan (positive control; 100 mg; $n = 2$). PECs were harvested 18 h after injection, and neutrophils were enumerated based on FACS analysis for $Ly6G^+Ly6B.2^+$ cells. (**B**) PEC neutrophils were enumerated and compared. Comparisons were performed using a Kruskal–Wallis with Dunn multiple comparison test. A p value <0.05 was considered significant.

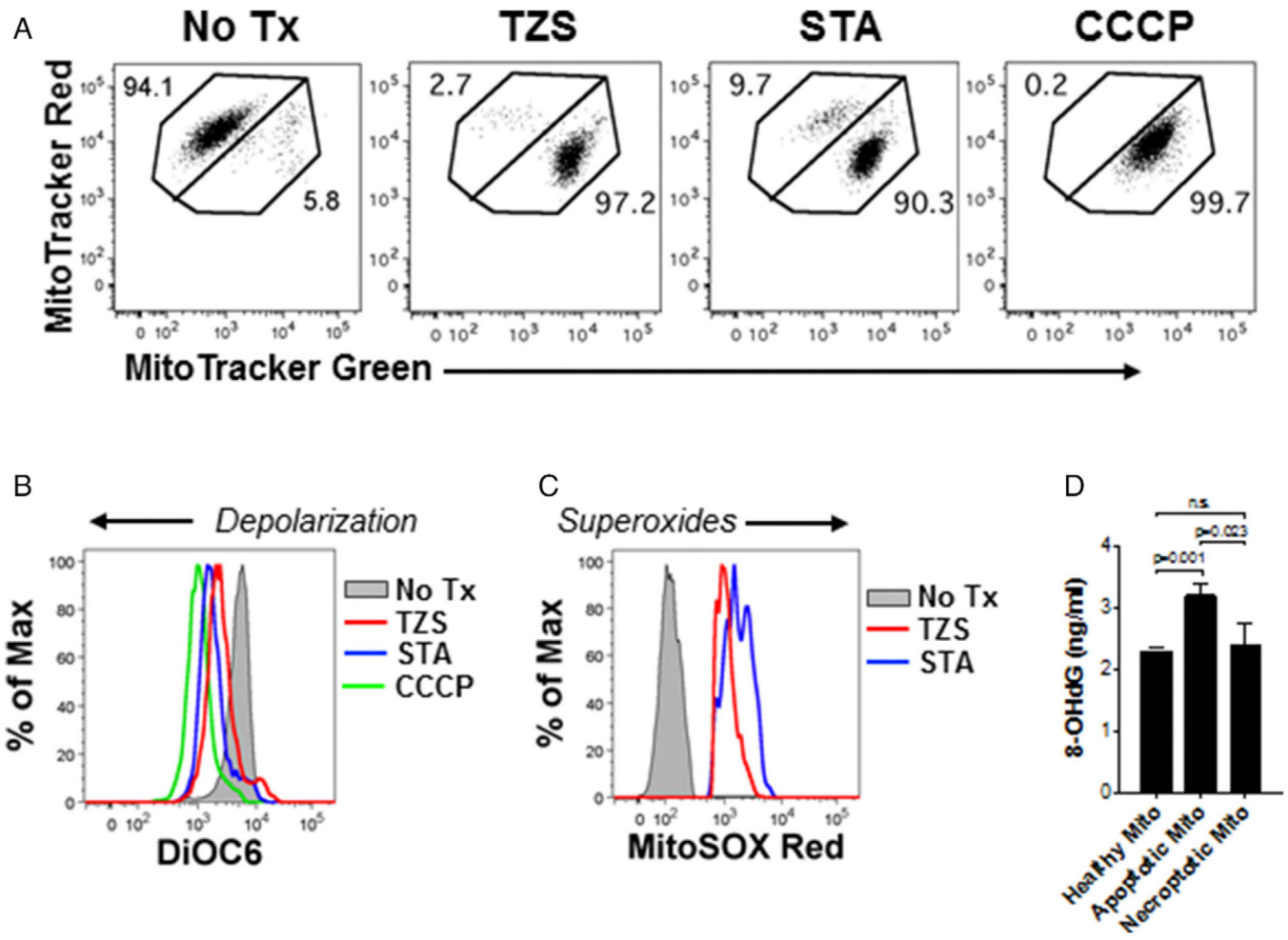

FIGURE 4. Apoptosis and necroptosis result in mitochondria dysfunction and injury.

L929 cells treated with STA (20 h) or TZS (6 h) were analyzed for loss of mitochondria membrane potential by costaining with MitoTracker Red and MitoTracker Green (**A**) or DiOC6 (**B**). Loss of red fluorescence intensity indicates depolarization. CCCP, a mitochondrial membrane depolarizing agent, was used as a positive control. (**C**) Superoxide production was measured with MitoSOX Red, producing a red fluorescence detectable by FACS. (**D**) mtDNA oxidation was determined by measuring the 8-OHdG content of DNA extracted from mitochondria of L929 cells treated with STA (20 h) or TZS (6 h). Comparisons were performed using a Kruskal–Wallis with Dunn multiple comparison test. A p value <0.05 was considered significant.

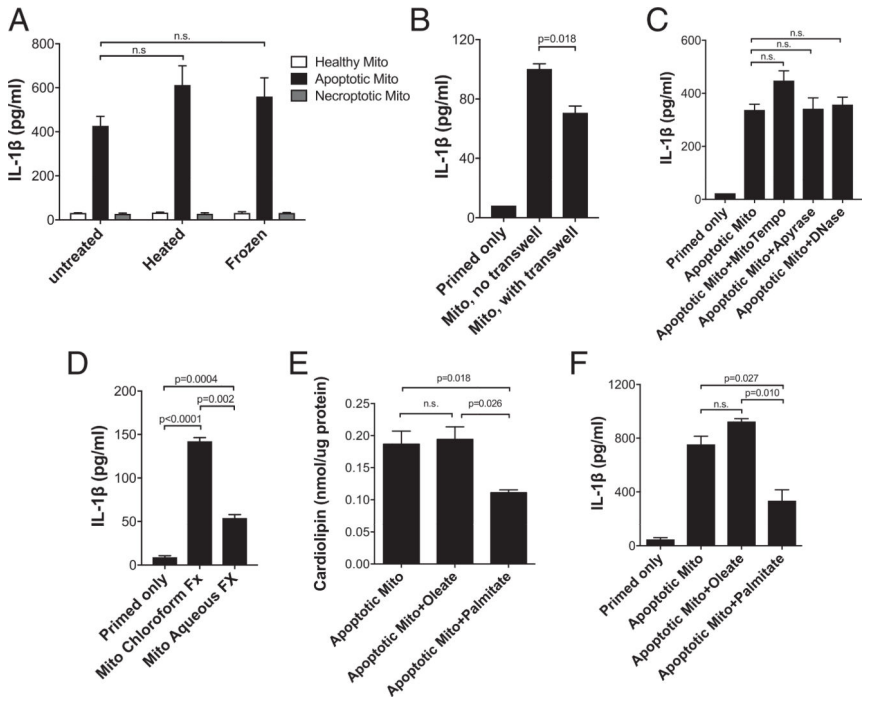

FIGURE 5. Mitochondrial cardiolipin plays a key role in macrophage inflammasome activation in response to apoptotic mitochondria.

LPS-primed J774A.1 cells were treated with mitochondria (100 mg/ml) under various conditions to determine which mitochondrial-derived molecules were responsible for inducing IL-1β production. (**A**) Neither heating mitochondria (100°C for 5 min) nor freezing mitochondria for (280°C for 2 h) affected IL-1β production. (**B**) Separating mitochondria from J744A.1 macrophages with a 0.4-mM filter significantly reduced IL-1β production. (**C**) Treatment with an antioxidant (MitoTEMPO), an ATPase (apyrase), or DNase had no significant effect on IL-1β production. (**D**) Following lipid extraction with chloroform, the chloroform fraction retained the majority of the IL-1β stimulation substance, suggesting involvement of a lipid. (**E**) Inhibition of cardiolipin synthesis with palmitate prior to the induction of apoptosis significantly decreased cardiolipin levels in mitochondrial preparations, compared with oleate (negative control). (**F**) Mitochondria purified from cells pretreated with palmitate prior to induction of apoptosis induced significantly lower IL-1β production, compared with oleate (negative control). Comparisons were performed using a Kruskal–Wallis with Dunn multiple comparison test. A p value <0.05 was considered significant.

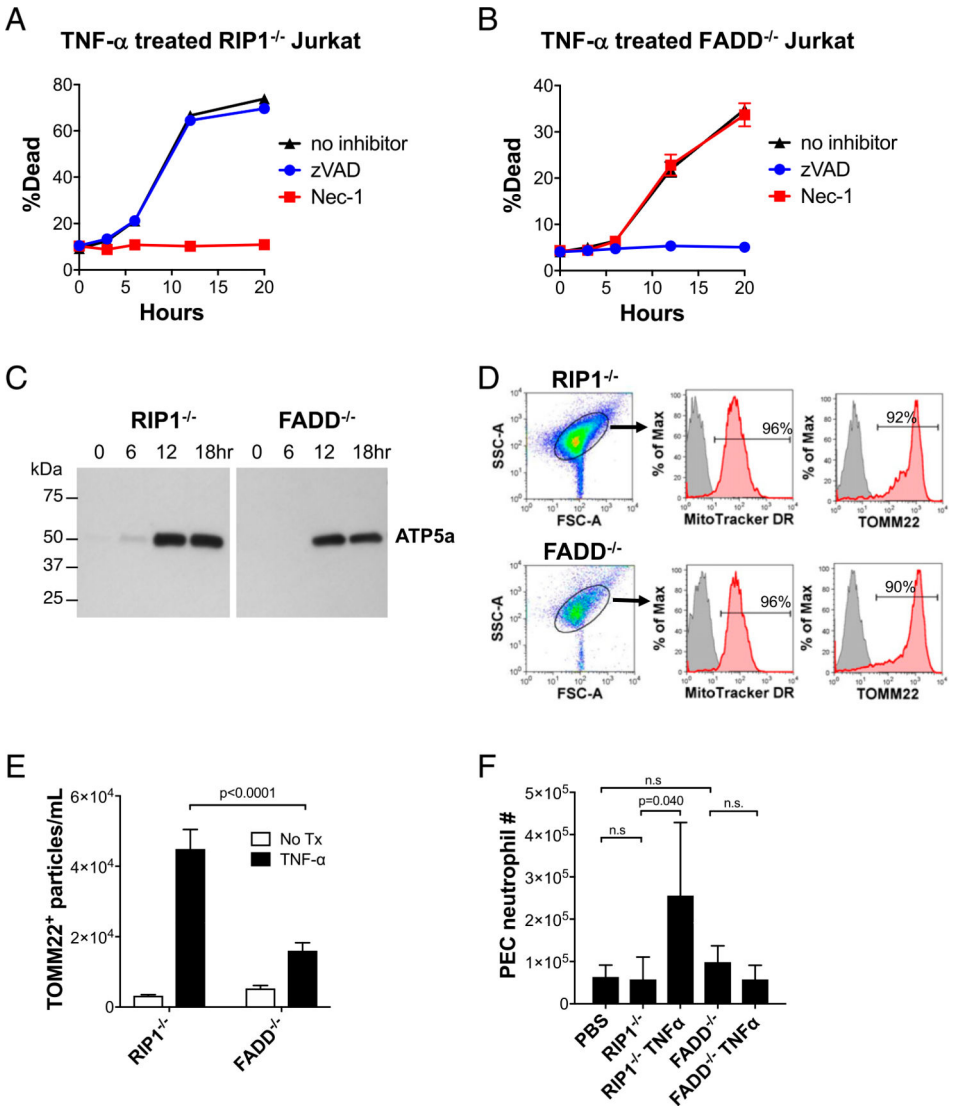

FIGURE 6. Human T cells undergoing apoptosis and necroptosis release mitochondria, and apoptotic mitochondria recruit neutrophils.

To repeat our findings using human cells, RIP1$^{-/-}$ and FADD$^{-/-}$ Jurkat cell lines were used. (**A** and **B**) Treatment with TNF-α causes both cell lines to undergo cell death. Use of inhibitors of apoptosis (zVAD) and necroptosis (Nec-1) demonstrate that RIP1$^{-/-}$ Jurkat cells specifically undergo apoptosis and that FADD$^{-/-}$ Jurkat cells specifically undergo necroptosis in response to TNF-α treatment. (**C** and **D**) Mitochondria are released by apoptotic and necroptotic Jurkat cells. Following TNF-α treatment of the Jurkat cell lines, the cell-free SN microparticles were collected, and their protein lysates were examined by Western blot analysis for ATP5a, a mitochondria-specific protein. SN microparticles were then stained with a mitochondria-specific dye, MitoTracker DR, and with anti-TOMM22 and FACS analyzed. Red shading indicates microparticles stained with MitoTracker DR or TOMM2, indicative of mitochondria. Gray shading indicates unstained microparticles (negative control). Horizontal lines indicate percentage of microparticles staining positively for MitoTracker DR or TOMM2, respectively. (**E**) Quantification of TOMM22^{+}

microparticles in the SN of TNF-α–treated Jurkat cell lines. (**F**) PEC neutrophil assay following i.p. mitochondria injection. C57BL/6 mice were injected with mitochondria (300 mg) purified from RIP1$^{-/-}$ or FADD$^{-/-}$ Jurkat cells that were untreated or treated with TNF-α. An equal volume of PBS (vehicle) was injected as a negative control. Eighteen hours after injection, PECs were harvested and analyzed for Ly6G^{+}Ly6B.2^{+} neutrophils by FACS ($n = 6$ for all conditions). Comparisons were performed using a Mann–Whitney U test (E) or a Kruskal–Wallis with Dunn multiple comparison test (F). A p value <0.05 was considered significant.

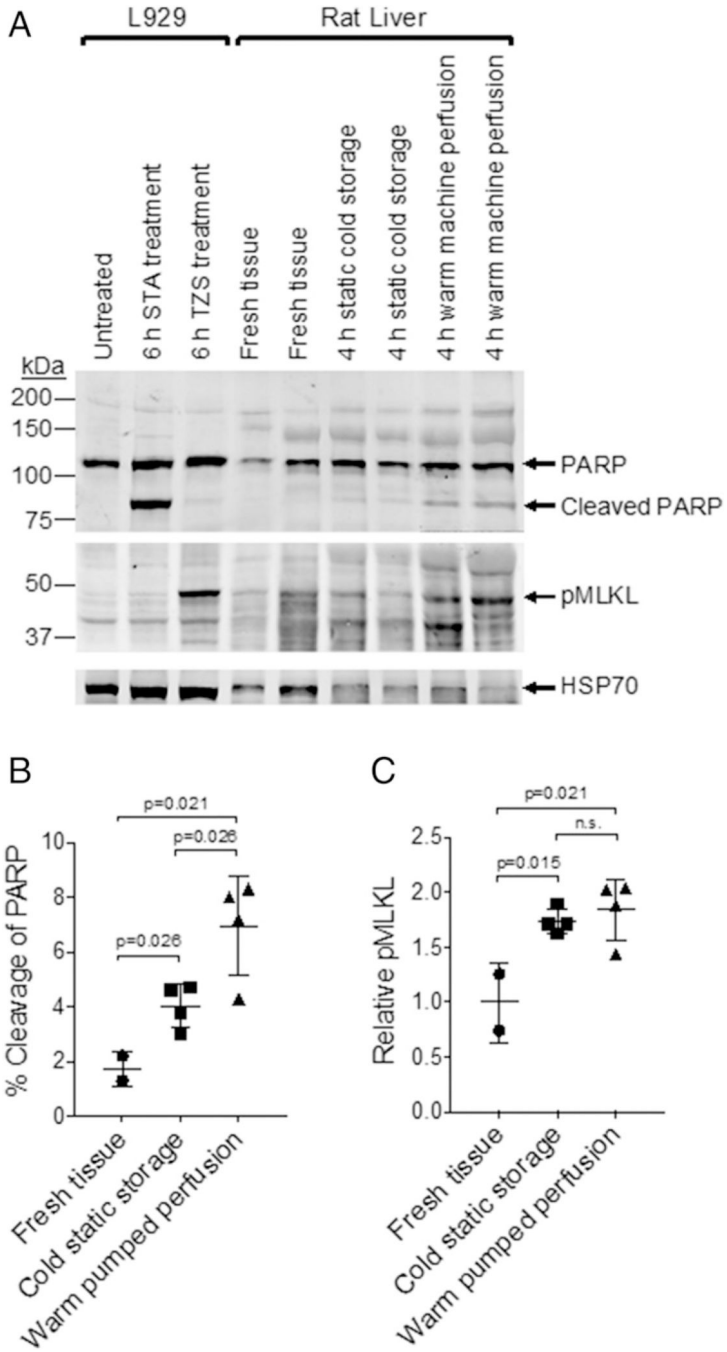

FIGURE 7. Apoptosis and necroptosis occur during simulated transplantation.

(**A**) Western blot analysis of L929 and rat liver tissue lysates were probed with anti-PARP and anti-pMLKL Abs. L929 cells treated for 6 h with STA or TZS were used as positive controls for apoptosis and necroptosis, respectively. Rat livers that were freshly procured (fresh tissue) served as negative controls. To mimic clinical transplantation, rat liver grafts were first stored for 4 h either by static cold preservation at 4°C or by warm machine perfusion at 37°C. Following organ storage, rat liver grafts underwent simulated transplantation by reperfusion with oxygenated Krebs–Henseleit buffer. Blots were reprobed

with anti-HSP70 Ab for protein loading control. Fresh samples were performed in duplicate and storage samples in quadruplicate, and the resulting bands on Western blot were quantified by digital densitometry. (**B**) Cleaved PARP was calculated by comparing the density of the cleaved PARP band with the uncleaved band. (**C**) Relative pMLKL was calculated by comparing the density of the Western blot band to the average density of the fresh liver pMLKL bands. Comparisons were performed using a Kruskal–Wallis with Dunn multiple comparison test. A p value <0.05 was considered significant.